The EMBO Journal Vol.17 No.2 pp.353–362, 1998

Three amino acids in the C-linker are major determinants of gating in cyclic nucleotide-gated channels

Xiangang Zong[1], Helmut Zucker[2], Franz Hofmann[1] and Martin Biel[1,3]

[1]Institut für Pharmakologie und Toxikologie, Technische Universität München, Biedersteinerstrasse 29, 80802 München and [2]Max-Planck-Institut für Psychiatrie, EDV-Gruppe, Am Klopferspitz 18a, 82152 Martinsried, Germany

[3]Corresponding author
e-mail: biel@ipt.med.tu-muenchen.de

The activation of cyclic nucleotide-gated (CNG) channels is a complex process comprising the initial ligand binding and a consecutive allosteric transition from a closed to an open configuration. The cone and olfactory CNG channels differ considerably in cyclic nucleotide affinity and efficacy. In each channel, the cyclic nucleotide-binding site is connected to the last transmembrane segment of the channel by a linker peptide (C-linker) of ~90 amino acids. Here we report that replacement of three amino acids in the cone C-linker by the corresponding amino acids of the olfactory channel (I439V, D481A and D494S) profoundly enhanced the cAMP efficacy and increased the affinities for cAMP and cGMP. Unlike the wild-type cone channel, the mutated channel exhibited similar single-channel kinetics for both cGMP and cAMP, explaining the increase in cAMP efficacy. We thus conclude that the identified amino acids are major determinants of channel gating.

Keywords: affinity/cAMP/cGMP/cyclic nucleotide-gated channel/gating

Introduction

Cyclic nucleotide-gated (CNG) channels comprise a multigene family of Ca^{2+}-permeable non-selective cation channels that are activated directly by the binding of cAMP or cGMP (Zufall *et al.*, 1994; Finn *et al.*, 1996; Zagotta and Siegelbaum, 1996). CNG channels were detected originally in photoreceptor (Fesenko *et al.*, 1985; Yau and Nakatani, 1985) and olfactory neurons (Nakamura and Gold, 1987), where they play key roles in transducing sensory information into changes in membrane potential. CNG channels have also been identified in a variety of non-sensory cells (Distler *et al.*, 1994; Biel *et al.*, 1995), including kidney (Ahmad *et al.*, 1992; Biel *et al.*, 1994; Karlson *et al.*, 1995), testis (Weyand *et al.*, 1994; Biel *et al.*, 1994), heart (Biel *et al.*, 1994; Ruiz *et al.*, 1996) and several parts of the brain (Dryer and Henderson, 1991; Bönigk *et al.*, 1996; Kingston *et al.*, 1996; Bradley *et al.* 1997; Sautter *et al.*, 1997). However, the physiological role of CNG channels is not known in most of these cells. Native CNG channels are supposed to have a tetrameric structure consisting of α and β subunits with unknown stoichiometry (Liu *et al.*, 1996; Varnum and Zagotta, 1996; for recent reviews, see Biel *et al.*, 1996; Finn *et al.* 1996). In contrast to the β subunits (Chen *et al.* 1993; Bradley *et al.*, 1994; Liman and Buck, 1994), the α subunits induce the formation of homomeric CNG channels when heterologously expressed in a variety of expression systems (Kaupp *et al.*, 1989; Dhallan *et al.*, 1990; Bönigk *et al.*, 1993; Biel *et al.*, 1994).

The olfactory CNG channel differs from rod and cone photoreceptor channels in its response to cyclic nucleotides (Zagotta and Siegelbaum, 1996): (i) it has a 15- to 100-fold higher apparent affinity for both cGMP and cAMP than the rod and cone channel and (ii) it is fully activated by cGMP and cAMP (i.e. cGMP and cAMP have the same efficacy for this channel) whereas cAMP acts as a partial agonist of photoreceptor channels activating only a fraction of the current induced by cGMP (i.e. cGMP has a higher efficacy than cAMP). CNG channel activation involves a complex cascade of conformational changes leading from closed to open channel configuration (Goulding *et al.*, 1994; Gordon and Zagotta, 1995b). In agreement with a cyclic allosteric model of channel activation, it recently has been demonstrated (Tibbs *et al.* 1997) that CNG channels transiently open in the absence of any cyclic nucleotide. Cyclic nucleotides strongly enhance channel activation by binding more tightly to the open state than to the closed state, thereby stabilizing the open conformation. Cyclic nucleotide binding takes place within a stretch of 130 amino acids in the carboxy-terminus (Kaupp *et al.*, 1989), which is homologous to the cyclic nucleotide-binding domain (CNBD) of protein kinases and the CAP protein of *Escherichia coli* (Shabb and Corbin, 1992). A threonine residue (T560) within the putative β7-roll (Altenhofen *et al.*, 1991) and a glutamic acid residue (D604) within the C-α helix (Varnum *et al.*, 1995) of the CNBD have been identified which critically affect the ligand-binding step and the cyclic nucleotide discrimination, respectively. However, since both amino acids are conserved in mammalian olfactory and photoreceptor channels, they cannot explain the differences observed in the response to cyclic nucleotides. Moreover, mutagenesis studies indicate that domains outside the CNBD, including the amino-terminus (Goulding *et al.*, 1994; Gordon and Zagotta, 1995b) and the cytoplasmatic linker connecting the sixth transmembrane segment (Broillet and Firestein, 1996, 1997), also influence CNG channel activation.

In the present study, we have investigated chimeric channels constructed between the bovine cone photoreceptor channel (CNG3; Biel *et al.*, 1994) and the rabbit olfactory channel (CNG2; Biel *et al.*, 1993) to narrow down sequences important for the different cAMP efficacies in both types of channels. Unlike previous studies, we used CNG3 instead of the rod channel (CNG1; Kaupp *et al.*,

1989) to construct chimeras since its structural and functional relationship to CNG2 is higher than that of CNG1. We expected that this closer relationship might circumvent intrinsic problems arising from combining domains of more distantly related proteins and thereby would allow single amino acids which are critical for channel activation to be pinpointed.

Results

Figure 1 shows the response of the CNG3 and CNG2 channel to cGMP and cAMP as measured in excised inside-out patches of transfected HEK293 cells. CNG3 differed in two major aspects from CNG2. (i) It was only partially activated by cAMP. The maximal current (I_{max}) induced by a saturating cAMP concentration corresponded to ~20% of the I_{max} induced by cGMP (Figure 1A and C, Table I). By contrast, CNG2 was fully activated by both cAMP and cGMP (Figure 1B and D, Table I). (ii) CNG 3 revealed a 15- to 20-fold lower apparent affinity than CNG2 for both cyclic nucleotides (Figure 1C and D, Table I). However, the ratio of the apparent affinities for cGMP and cAMP, which is a measure of the ligand selectivity, was comparable for both channels (CNG2: $K_{a[cAMP]}/K_{a[cGMP]} = 57$; CNG3: $K_{a[cAMP]}/K_{a[cGMP]} = 87$; see Table I). To confirm that cAMP acted as a partial agonist in CNG3 and a full agonist in CNG2, we measured the dose–response curves of cGMP alone and in combination with fixed concentrations of cAMP (Figure 1E and F). As expected for a competitive interaction between a partial and a full agonist, cAMP inhibited the current of CNG3 that would have been elicited by subsaturating concentrations of cGMP (Figure 1E). The inhibition depended on the concentration of cAMP. For example, the current induced by 30 μM cGMP, which corresponds to ~90% of I_{max}, was reduced by 1 mM cAMP to ~65% of I_{max} whereas it was reduced to 50% of I_{max} by 2 mM cAMP. By contrast, cAMP and cGMP responses were additive for the CNG2 channel, which indicated that both ligands were full agonists of this channel (Figure 1F).

Identification of amino acid residues affecting cAMP efficacy

To identify channel domains responsible for the different cAMP efficacies of CNG2 and CNG3, we constructed chimeric channels based on the CNG3 transmembrane core and variable parts of CNG2. As a measure of the relative cAMP efficacy (E_{cAMP}), we determined the ratio of the currents obtained at saturating concentrations of cAMP and cGMP (I_{cAMP}/I_{cGMP}). In an initial round of mutations, we replaced large parts of CNG3 with the corresponding sequences of CNG2 (Figure 2; Table I). Replacement of the cytoplasmic amino-terminal segment (Ch2) did not substantially change E_{cAMP}, whereas the replacement of the complete carboxy-terminus, which includes the CNBD and the linker between the S6 segment and the CNBD (C-linker), resulted in a chimera (Ch3) which was fully activated by cAMP. Replacement of both amino- and carboxy-termini did not alter E_{cAMP} with respect to Ch3. The replacement of CNG3 channel domains by corresponding CNG2 domains did not alter the voltage dependence of channel activation. The ratio of currents evoked at –60 mV and +60 mV was ~0.8, which is identical to the value reported for the wild-type CNG3 channel (Biel *et al.*, 1994). We next subdivided the carboxy-terminus of Ch3 into two parts. Ch8 contains only the C-linker and the first part of the CNBD which is highly conserved between CNG2 and CNG3 (only three exchanges; see Figure 3A). The complementary chimera (Ch9) contains the CNBD and the carboxy-terminal end of CNG2. The currents of both chimeras are shown in

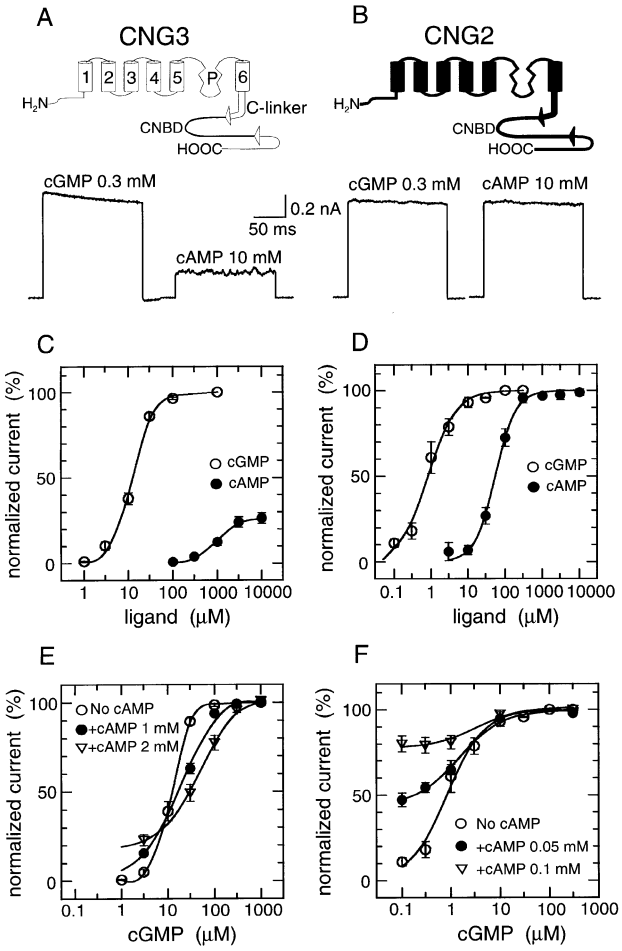

Fig. 1. Differential activation of CNG2 and CNG3 by cyclic nucleotides. (A and B) Top: transmembrane folding model of the CNG3 (**A**) and CNG2 channel (**B**). The transmembrane segments (1–6), the pore region (P) and the cyclic nucleotide-binding domain (CNBD) are indicated. The C-linker connects the S6 segment with the CNBD. Bottom: current traces of CNG3 (A) and CNG2 (B) induced in excised inside-out patches by saturating concentrations of cGMP and cAMP. The membrane potential was +60 mV. (C and D) Dose–response curves of CNG3 (**C**) and CNG2 (**D**) for cGMP (○) and cAMP (●). The curves were calculated from the Hill equation with the following parameters: activation of CNG3 by cGMP, $\nu = 1.65$, $K_a = 12.5$ μM ($n = 11$), by cAMP, $\nu = 1.78$, $K_a = 995$ μM ($n = 14$); activation of CNG2 by cGMP, $\nu = 1.57$, $K_a = 0.83$ μM ($n = 15$), by cAMP, $\nu = 1.56$, $K_a = 55$ μM ($n = 17$). (E and F) Dose–response curves of CNG3 (**E**) and CNG2 (**F**) for cGMP alone (○) and in the presence of 1 or 0.05 mM (●) and 2 or 0.1 mM (▽) of cAMP. Solid lines for current activation in the presence of both ligands were calculated with the Dean equation (see Materials and methods) with the following parameters: for CNG3 at 1 mM cAMP, $K_a = 17.9$ μM, $K_b = 2012$ μM, $\alpha = 1.02$, $\beta = 0.15$ ($n = 7$); at 2 mM cAMP, $K_a = 21.3$ μM, $K_b = 1520$ μM, $\alpha = 1.03$, $\beta = 0.26$ ($n = 8$); for CNG2 at 0.05 mM cAMP, $K_a = 0.83$ μM, $K_b = 64.5$ μM, $\alpha = 0.99$, $\beta = 1.00$ ($n = 8$); at 0.1 mM cAMP, $K_a = 0.97$ μM, $K_b = 49.2$ μM, $\alpha = 1.00$, $\beta = 1.03$ ($n = 5$). The fits for activation by cGMP alone were taken from (C) and (D).

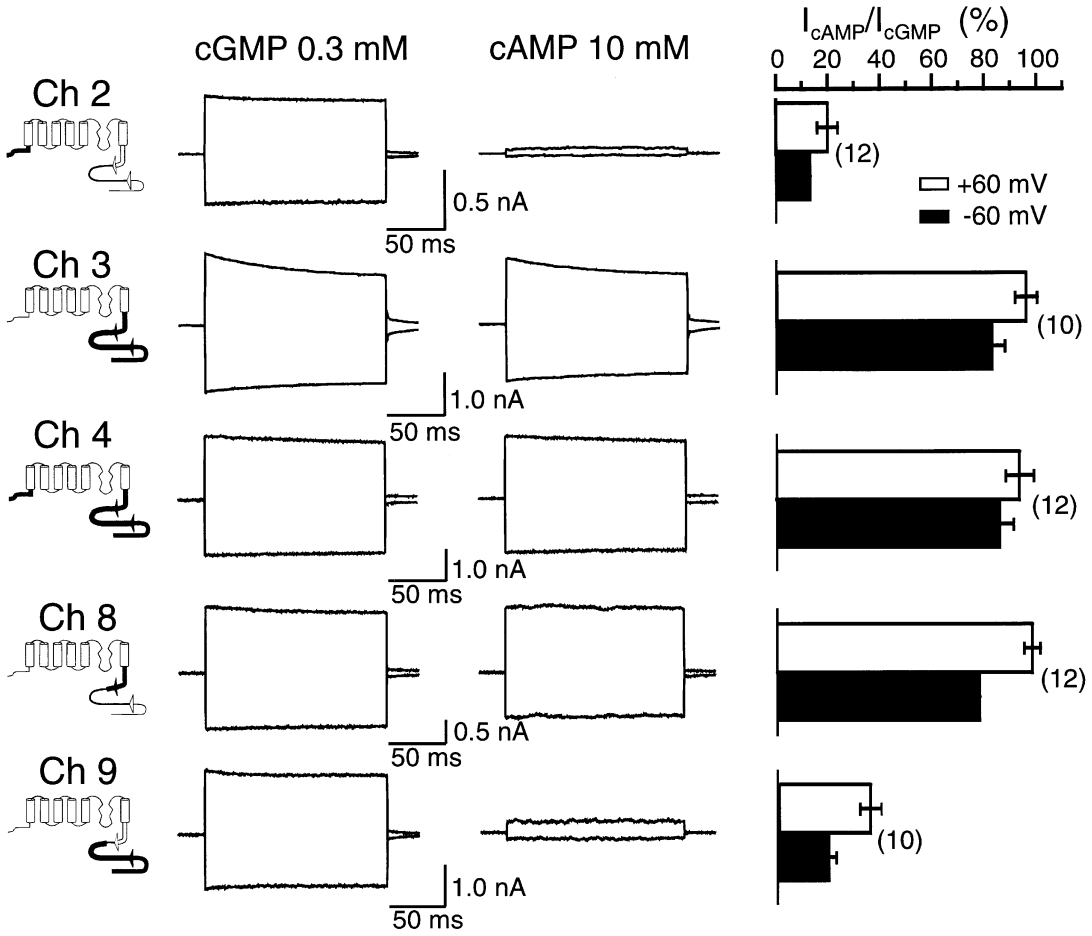

Fig. 2. The C-linker determines the efficacy of cAMP. Left panel: schematic representation of the chimeras 2, 3, 4, 8 and 9. Channel domains originating from CNG3 are illustrated by thin white lines, domains derived from CNG2 are shown by thick black lines. Middle panel: current traces of the chimeras induced by saturating concentrations of cGMP and cAMP at ±60 mV. Right panel: ratio between the current amplitudes elicited by saturating concentrations of cAMP and cGMP.

Table I. Ratio of maximal currents measured in the presence of saturating concentrations of cAMP (I_{cAMP}) and cGMP (I_{cGMP}) and apparent ligand affinities (K_a) of wild-type and chimeric CNG channels

Channels	I_{cAMP}/I_{cGMP} (%)	K_a (μM)		$K_{a(cAMP)}/K_{a(cGMP)}$
		cGMP	cAMP	
CNG3	18.9 ± 1.64 (19)	12.6 ± 0.92 (11)	1095 ± 80 (14)	87
CNG2	101 ± 0.76 (11)	0.90 ± 0.21 (15)	50.9 ± 9.0 (17)	57
Ch2	19.9 ± 3.95 (20)	11.4 ± 2.08 (12)	595 ± 35 (12)	52
Ch3	95.6 ± 4.16 (10)	5.80 ± 1.02 (11)	239 ± 31 (6)	41
Ch4	93.3 ± 5.18 (12)	2.65 ± 0.43 (12)	61.8 + 8.6 (11)	23
Ch8	98.1 ± 3.04 (12)	2.53 ± 0.31 (8)	305 ± 53 (7)	120
Ch9	35.1 ± 3.83 (10)	13.2 ± 2.42 (7)	512 ± 31 (8)	39
Ch12	77.6 ± 2.27 (18)	4.64 ± 0.60 (8)	534 ± 64 (7)	115
Ch13	42.2 ± 3.80 (13)	9.86 ± 0.75 (8)	nd	nd
Ch20	37.1 ± 2.66 (16)	10.7 ± 1.35 (6)	nd	nd
Ch21	81.0 ± 2.73 (12)	3.45 ± 0.42 (8)	nd	nd
Ch24	81.1 ± 2.73 (13)	6.17 ± 0.56 (9)	nd	nd
Ch25	70.4 + 4.94 (12)	8.85 ± 0.51 (10)	482 ± 35 (7)	55
Ch26	46.5 ± 3.95 (10)	7.24 ± 0.45 (9)	nd	nd
Ch28	57.3 ± 2.98 (11)	5.14 ± 0.55 (7)	nd	nd
Ch30	80.5 ± 1.96 (13)	4.97 ± 0.38 (10)	625 ± 52 (13)	126
Ch35	60.0 ± 4.83 (8)	nd	790 ± 50 (8)	nd
Ch36	83.6 ± 2.20 (7)	nd	435 ± 44 (7)	nd
Ch37	88.0 ± 2.89 (8)	nd	429 ± 55 (13)	nd
Ch38	91.8 ± 4.59 (4)	nd	657 ± 41 (7)	nd

I_{cAMP} and I_{cGMP} were measured at +60 mV in the presence of 10 mM cAMP and 0.3 mM cGMP, respectively. The K_a values were taken at +60 mV by fits to the Hill equation. Numbers in parentheses indicate the number of patches tested. nd, not determined.

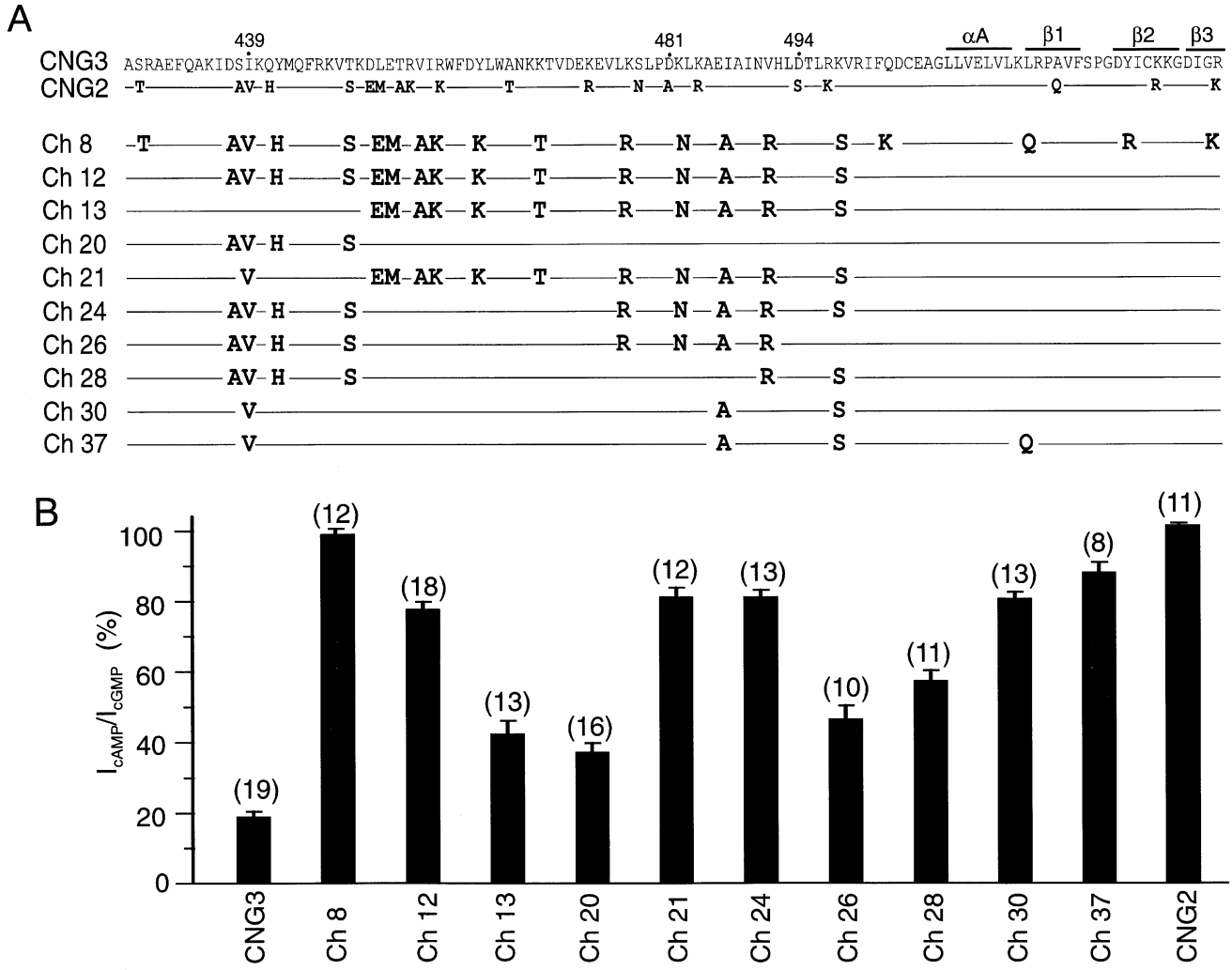

Fig. 3. Three amino acids within the C-linker are major determinants of cAMP efficacy. (**A**) Comparison of the sequence of the C-linker and the first part of the CNBD (A-α helix to β3-roll) of wild-type CNG3 and CNG2 channels and CNG channel chimeras. The numbering refers to the sequence of CNG3. In CNG2 and chimeras Ch8–Ch37, only those amino acids are shown which differ from the sequence of CNG3. Black lines indicate sequence identities with CNG3. (**B**) Ratio of the current amplitudes induced by saturating concentration of cAMP and cGMP at +60 mV for wild-type and chimeric CNG channels.

Figure 2. Ch8 was activated equally well by cAMP and cGMP (E_{cAMP} = 0.98) whereas Ch9 was only activated slightly better by cAMP than was CNG3. Similarly to Ch3, Ch8 revealed a significant increase in the apparent affinity for both cAMP and cGMP (Table I). By contrast, the exchange of amino- and carboxy-terminal sequences between CNG2 and CNG3 did not alter the ligand selectivity substantially. However, chimeras containing the olfactory amino-terminus (Ch2), the olfactory CNBD (Ch3, Ch9) or both domains of the olfactory channel (Ch4) revealed, similarly to the wild-type CNG2 channel, a somewhat smaller difference in K_a (~20- to 60-fold) than the wild-type CNG3 channel (90-fold) and Ch8 (120-fold) (see Table I). Taken together, these results suggested that the amino-terminus and the CNBD of CNG2 increased apparent ligand affinities and weakened the ligand discrimination but had only a small influence on E_{cAMP}. On the other hand, the high E_{cAMP} of Ch8 clearly indicated that the major determinant of E_{cAMP} was localized within the C-linker.

Figure 3A shows the sequence of the C-linker and the first part of the CNBD of CNG3 compared with the corresponding sequence of CNG2 which is present in Ch8. In total, there are 20 amino acid residues exchanged, 17 residues within the C-linker and three within the CNBD, two of which are conservative exchanges (K530R and R536K). To identify single amino acids affecting E_{cAMP}, we systematically replaced amino acid stretches or single residues of Ch8 with the corresponding sequences of CNG3. The sequences of some of the resulting chimeric channels are shown in Figure 3A. All constructed chimeras were expressed reasonably well. The ratio of I_{cAMP}/I_{cGMP} as a parameter for E_{cAMP} is shown in Figure 3B and Table I. We first reduced the size of the exchanged sequence with respect to Ch8. Ch12 differs from Ch8 in that it has only exchanged the C-linker of CNG3 against that of CNG2 whereas the complete CNBD of CNG3 is present. This reduction slightly decreased E_{cAMP} from 0.98 to ~0.8, suggesting that the influence of the CNBD is small. By contrast, Ch13, which is distinguished from Ch12 only by a difference in the first four amino acids, revealed a strongly reduced E_{cAMP} (0.42). The difference in E_{cAMP} between Ch12 and Ch13 could be attributed completely to the exchange of I439V. Ch21, which is identical

to Ch13 but additionally contains the I439V exchange, revealed the same E_{cAMP} as Ch12 (~0.8). The three other residues (S428, A438 and Q441) had no influence on channel activation by cAMP. The I439V exchange was necessary but not sufficient to explain the high E_{cAMP} of Ch12, since Ch20, which contains this exchange but lacks the C-terminal half of the C-linker, revealed a strongly reduced E_{cAMP} (0.37) with respect to Ch12. Extensive investigation of a variety of chimeras resulted in the identification of two additional amino acids within the C-linker (D481A and D494S) which also participate in determining E_{cAMP}. Ch30, which differs from the wild-type CNG3 channel only by three exchanges (I439V, D481A and D494S), revealed the same E_{cAMP} (~0.8) as Ch12. All three exchanges were necessary in combination since the omission of any of the exchanges resulted in a significant reduction in E_{cAMP} (see Ch26, Ch28 and Ch35 in Figure 3 and Table I). We next tried to increase E_{cAMP} further by systematically exchanging the five amino acids in Ch30 which vary between Ch8 (E_{cAMP} = 0.98) and Ch12 (E_{cAMP} = 0.8). However, the remaining difference in E_{cAMP} could not be attributed to a single residue. The biggest effect was seen with the exchange of A520Q (Ch37) in the β1-roll of the CNBD which resulted in an additional 10% increase in E_{cAMP} (E_{cAMP} = 0.88).

Functional properties of Ch30

Since the exchange of three amino acids in the CNG3 C-linker giving rise to Ch30 represented the minimal requirement for the induction of high E_{cAMP}, we subsequently analysed this chimera in more detail. E_{cAMP} is defined as the ratio of I_{max} at saturating concentrations of cAMP and cGMP. Thus, the increase in E_{cAMP} may result from a relative decrease in the maximal cGMP current of Ch30 with respect to that of CNG3. We could exclude this possibility since the maximal cGMP current was not significantly different ($P > 0.05$) between CNG3 (I_{max} = 749 ± 119 pA, range 60–2250 pA, n = 19) and Ch30 (I_{max} = 589 ± 143 pA, range 105–1680 pA, n = 13). The increase in E_{cAMP} could also be explained by other mechanisms, including an increase in the cAMP affinity, the alteration of the voltage dependence of channel opening or changes in the channel gating process. Figure 4 shows that changes in ligand affinity and voltage dependence are unlikely to explain the strong enhancement of the cAMP-induced current observed in Ch30 (Figure 4A). Ch30 revealed a slight increase in the apparent affinity for cAMP with respect to CNG3 (Figure 4B, Table I); however, an even bigger increase in affinity was seen for cGMP, resulting in a similar affinity ratio of both channels ($K_{a[cAMP]}/K_{a[cGMP]}$ was 87 for CNG3 and 125 for Ch30). As has been shown for CNG2 and CNG3, cGMP and cAMP competed for the same binding site in Ch30 (Figure 4C). The major difference between CNG3 and Ch30 consisted of the increase in E_{cAMP} changing cAMP from a partial to a nearly full agonist. Finally, the shape of the current–voltage relationship curves was not substantially changed between Ch30 (Figure 4D) and CNG3 (Figure 4E), indicating that the three amino acid exchanges present in Ch30 did not affect the voltage dependence of channel activation.

Single-channel analysis of Ch30

The above results suggested that the mutations in the C-linker might affect channel gating. We therefore measured the single-channel current of Ch30 and compared it with the current of CNG2 and CNG3 (Figure 5; Table II). The single-channel current of CNG3 induced by cGMP and cAMP revealed prominent differences (Figure 5A). With cGMP, two kinds of opening events were visible, a very brief opening mode with an open time constant of <1 ms and a long opening mode with a time constant of ~5 ms. By contrast, when the current was activated by cAMP, only brief openings were present. At high concentrations of cAMP, the opening of multiple channels was observed (Figure 5A, sixth trace) whereas long openings did not occur. This finding suggested that the ligand specificity of the opening modes is an intrinsic property of the CNG3 channel and does not depend on the ligand concentration.

The single-channel current of the CNG2 channel was identical with both ligands (Figure 5B). It was characterized by very long openings which were at least three times as long as those observed with CNG3. In addition, brief openings similar to those observed in CNG3 were also present. The amplitude of the CNG2 single-channel current did not depend on the activating ligand (I_{cAMP} = 3.15 ± 0.08 pA; I_{cGMP} = 3.02 ± 0.08 pA at +60 mV; n = 3) but differed slightly from that of CNG3 (I_{cAMP} = 2.46 ± 0.07 pA; n = 3; I_{cGMP} = 2.42 ± 0.06 pA; n = 3), most likely reflecting the presence of different pore regions in both channels. Figure 5C shows single-channel currents recorded from Ch30. The opening mode was very similar for both cyclic nucleotides, and closely resembled that of the cGMP-activated CNG3 channel. It was characterized by a mixture of very brief and longer opening events. Thus, Ch30 resembled CNG2 on the single-channel level in that it did not discriminate between cGMP and cAMP. However, Ch30 differed from CNG2 in that the very long opening events which are typical for CNG2 were absent. In addition, the amplitude of the single-channel current of Ch30 corresponded to that of CNG3 (I_{cAMP} = 2.40 ± 0.06 pA; I_{cGMP} = 2.39 ± 0.05 pA at +60 mV; n = 3), reflecting the presence of the same pore region in both channels. From these results, we concluded that the exchange of three amino acids giving rise to Ch30 increased E_{cAMP} by allowing longer openings in the presence of cAMP.

Inhibitory effect of the CNG3 C-linker on the CNG2 current

If the C-linker of CNG2 increases E_{cAMP} when introduced into CNG3, the replacement of the C-linker of CNG2 with the corresponding sequence of CNG3 should conversely diminish E_{cAMP}. Figure 6 shows currents activated in the reverse chimera 25 (Ch25) which is based on the CNG2 core but contains the C-linker of CNG3. As expected, Ch25 discriminated between the cyclic nucleotides, being only partially activated by cAMP (Figure 6A). However, the effect of the C-linker was less than in the opposite case, leading to a reduction of E_{cAMP} from 1.0 in CNG2 to 0.7 in Ch25. In parallel to the decrease in E_{cAMP}, Ch25 exhibited a 10-fold decrease in apparent affinities for both cGMP and cAMP, bringing the K_a values of Ch25 and Ch30 for cGMP and cAMP close to each other (Table I). The inhibitory influence of the CNG3 C-linker could also

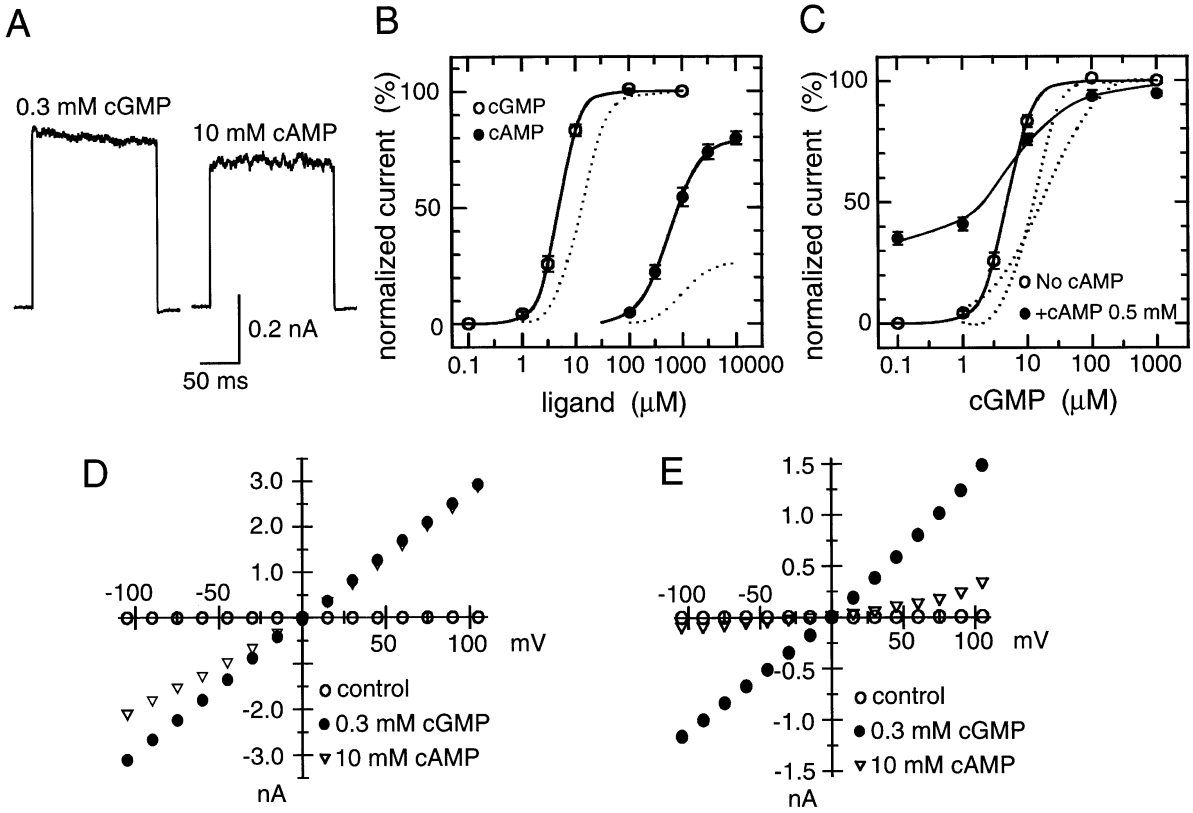

Fig. 4. Functional properties of the Ch30. (**A**) Current traces of Ch30 induced by saturating concentrations of cGMP and cAMP at +60 mV. (**B**)Dose–response curves for cGMP (○) and cAMP (●). The curves were fitted with the Hill equation using the following parameters. cGMP, $\nu = 2.18$, $K_a = 4.83$ μM, cAMP, $\nu = 1.56$, $K_a = 581$ μM. The dotted lines represent dose–response curves for cGMP and cAMP of the wild-type CNG3 channel. (**C**) Dose–response curves of Ch30 for cGMP alone (○) and in the presence of 0.5 mM cAMP (●). The solid lines for current activation in the presence of 0.5 mM cAMP are best fits of the Dean equation using the following parameters: $K_a = 2.9$ μM, $K_b = 782$ μM, $\alpha = 0.96$, $\beta = 0.83$. The curve of cGMP alone was taken from (B). For comparison, the dose–response curves of the CNG3 channel for activation by cGMP and by a combination of cGMP + 1 mM cAMP are included as dotted lines. (D and E) Current–voltage relationships of Ch30 (**D**) and CNG3 (**E**).

be demonstrated at the single-channel level (Figure 6B). As can be seen clearly from the current traces, the presence of the CNG3 C-linker significantly reduced the open time for cAMP with respect to that observed with cGMP. In particular, the very long openings which are typical for the wild-type CNG2 channel were completely missing in Ch25.

Discussion

In this study, we provide evidence that the linking region (the C-linker) connecting the last transmembrane domain with the CNBD of CNG channels is an important determinant of channel activation. The replacement of the cone (CNG3) channel C-linker by that of the olfactory (CNG2) channel resulted in a chimera (Ch8) which, like the olfactory channel, was almost equally well activated by cAMP and cGMP, whereas the wild-type cone channel is only poorly activated by cAMP. Conversely, the reverse chimera (Ch25) containing the cone C-linker within an olfactory channel backbone revealed a significantly reduced efficacy of channel activation by cAMP. The increase and decrease in the cAMP efficacy in Ch8 and Ch25, respectively, was paralleled by an increase and decrease in the apparent affinities for both cAMP and cGMP but not by a substantial change in the ligand selectivity, suggesting that the C-linker affects the channel gating process. The exchange of the CNBD and the cytoplasmic amino-terminus slightly increased the apparent cAMP affinity but had no major influence on the cAMP efficacy (E_{cAMP}). This finding contrasts with recent studies on the activation of chimeras constructed between the rod photoreceptor and the olfactory channel, which identified the amino-terminus and the first two transmembrane segments of the channel as being especially influential in affecting channel activation (Goulding *et al.*, 1994; Gordon and Zagotta, 1995b). This discrepancy could arise from the fact that cone and olfactory channels are both structurally and functionally more related to each other than are rod and olfactory channels. Thus, the amino-termini of cone and olfactory channels might be functionally equivalent whereas those of rod and olfactory channels are not. The finding that the C-linker has no major influence on the ligand selectivity is in line with the recent studies showing that an aspartate residue within the C-α helix of the CNBD (Varnum *et al.*, 1995), which is present in both the cone and olfactory channel, is the major determinant of ligand discrimination. It is noteworthy that the replacement of D604 by a neutral amino acid (Varnum *et al.*, 1995) completely converts the ligand selectivity and efficacy of the rod channel from a cGMP to a highly cAMP-specific channel. However, this mutation also induces an ~5-fold decrease in the apparent affinity for cGMP (Varnum and Zagotta, 1996). Thus the effect of

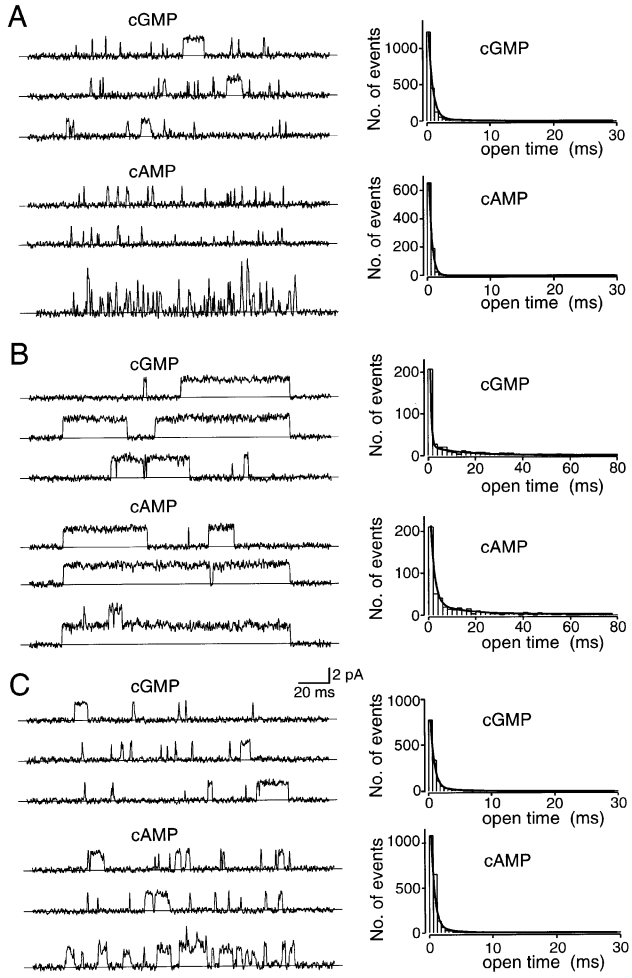

Fig. 5. Single-channel currents of CNG3 (**A**), CNG2 (**B**) and Ch30 (**C**) recorded at +60 mV. Left panels: current traces induced in the same patch by cGMP (cGMP concentrations: A, 1 μM; B, 0.1 μM; C, 0.3 μM) or cAMP (cAMP concentrations: A, 100 μM; B, 10 μM; C, 30 μM). For each channel, the third current trace for cAMP was recorded in the presence of a high concentration of cAMP (cAMP concentrations: A, 300 μM; B, 100 μM; C, 300 μM). The continuous lines indicate the closed state of the respective channels. Right panels: open time distribution of currents activated by cGMP and cAMP for CNG3 (A), CNG2 (B) and Ch30 (C). The cGMP concentrations were the same as used in the left panel. cAMP was used at the low concentration as shown in the left panel. The open times were fitted by two exponentials for all currents, with the exception of the CNG3 current induced by cAMP, which was fitted by one exponential (for values of time constants see Table II).

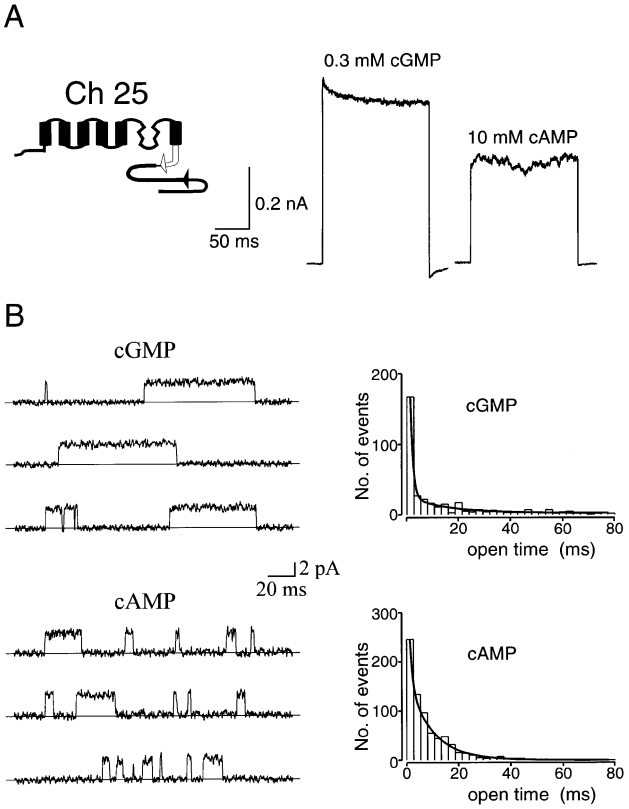

Fig. 6. Activation of the inverse chimera (Ch 25) by cGMP and cAMP. (**A**) Left: schematic representation of Ch25. The C-linker and the first part of the CNBD originating from CNG3 are illustrated in white. Right: current traces induced by saturating concentrations of cGMP and cAMP at +60 mV. (**B**) Left panels: single-channel currents induced in the same patch by 3 μM cGMP and 100 μM cAMP at +60 mV. Right panels: open time distribution of the current induced by 3 μM cGMP and 100 μM cAMP. The solid lines represent the best fit by two exponentials. The time constants were as follows: for cGMP: τ_{o1} = 1.03 ms, τ_{o2} = 14.5 ms; for cAMP: τ_{o1} = 1.03 ms, τ_{o2} = 9.40 ms.

the C-linker and the C-α helix on E_{cAMP} might be conferred by different molecular mechanisms.

By extensive mutational analysis, we identified three amino acids within the cone C-linker that when replaced by the corresponding amino acids of the olfactroy channel (I439V, D481A and D494S) confer most of the observed increase in E_{cAMP}. All three exchanges are needed in combination to achieve high E_{cAMP}, since the replacement of any of these residues by the corresponding residues of the cone channel leads to a significant decrease in E_{cAMP} (see E_{cAMP} of Ch30 versus E_{cAMP} of Ch26, 28 and 35). The remaining difference between the E_{cAMP} of Ch8 and Ch30 could not be attributed to single amino acids. Thus, the complete olfactory C-linker and the β1-roll of the olfactory CNBD may be necessary to achieve full activation of the channel by cAMP. The three amino acids identified are not adjacent to each other but rather are dispersed over the primary sequence of the C-linker. However, in the three-dimensional structure of the region, all three amino acids might be in close contact with each other, forming a highly ordered structure which is disrupted by mutating any of the residues. Interestingly, two of the exchanges (D481A and D494S) which increase E_{cAMP} result in the removal of negative charge from the C-linker, suggesting that electrostatic interactions might be involved in the channel activation process. It should be noted that the rod photoreceptor channel which is also very poorly activated by cAMP also contains negative charges at equivalent positions (Kaupp *et al.*, 1989). Val439 is localized in close proximity to two histidines in rod (H420 in rat rod channel) and olfactory channels (H394 in rabbit CNG2) which have been identified as the molecular target of the potentiation (Gordon and Zagotta, 1995a) or inhibition (Gordon and Zagotta, 1995b) of the respective channels by Ni^{2+}. In CNG3, both histidines are changed to glutamine residues. Mutation of Q441 in CNG3 to histidine as present in the olfactory channel had no effect on E_{cAMP} and apparent ligand affinities (not shown). Likewise, the reverse mutation in the olfactory channel

Table II. Single-channel kinetics of CNG channels

Channels/ligand	Time constants (ms)			
	τ_{o1}	τ_{o2}	τ_{c1}	τ_{c2}
CNG2/cGMP	0.88 ± 0.14	13.7 ± 1.11	0.94 ± 0.28	29.6 ± 6.49
CNG2/cAMP	0.75 ± 0.11	11.9 ± 0.82	0.97 ± 0.39	31.8 ± 7.67
CNG3/cGMP	0.72 ± 0.06	4.55 ± 0.58	1.92 ± 0.70	26.2 ± 10.6
CNG3/cAMP	0.48 ± 0.05	–	2.31 ± 0.45	24.1 ± 7.08
Ch30/cGMP	0.57 ± 0.01	3.34 ± 0.37	2.30 ± 0.56	17.8 ± 1.37
Ch30/cAMP	0.54 ± 0.02	2.71 ± 0.24	1.90 ± 0.81	13.7 ± 1.52

Time constants for open (τ_{o1}, τ_{o2}) and closed (τ_{c1}, τ_{c2}) states were fitted from open and closed time distributions as shown in Figure 5. For each channel, three individual patches were measured.

(H394Q) also did not alter channel activation parameters (not shown). From these results, it can be concluded that the respective region of CNG channels containing the histidine residues critically affects channel activation but that the histidines themselves are not important for 'normal' channel activation by cAMP or cGMP. The importance of the C-linker in the process of channel activation is also underlined by the recent finding (Broillet and Firestein, 1996, 1997) that covalent modification of a cysteine residue (C505 in CNG3) by NO and alkylating agents leads to a long-term activation of the channel in the absence of cyclic nucleotides. Since C505 is present in both photoreceptor and olfactory channels, it cannot explain the differences in E_{cAMP}. Nevertheless, C505 may fulfil an important and highly conserved role in the gating process of CNG channels.

Mechanism of increase in E_{cAMP}

The currents measured at saturating concentrations of cGMP were in the same range for both the wild-type CNG3 channel and Ch30. This finding makes it very likely that the observed increase in E_{cAMP} in Ch30 is not due to a decrease in the cGMP efficacy but rather results from an increase in the maximal current at a saturating cAMP concentration. In agreement with this interpretation, the E_{cAMP} values obtained from measurement of I_{max} at saturating concentrations of either cGMP or cAMP alone could be verified by fitting the dose–response curves for activation of CNG3 and Ch30 by fixed combinations of cGMP and cAMP (Figures 1E and 4C). It should be noted that the use of current ratios is not equivalent to the determination of maximal open probabilities at saturating ligand concentrations, which would require a noise analysis of the respective channels (Goulding *et al.*, 1994). However, the error introduced by the use of current ratios may be small and should not significantly affect the general conclusions drawn from our data.

Inspection of the single-channel currents of wild-type channels and Ch30 revealed a possible mechanism explaining the increase in E_{cAMP} observed in Ch30. The single-channel current of the cone and the olfactory channel was characterized by the presence of brief ($\tau < 1$ ms) and much longer openings (τ 3–14 ms, depending on channel type and agonist), which is consistent with reports describing similar opening modes in expressed homomeric CNG channels (Kaupp *et al.*, 1989; Goulding *et al.*, 1992). The single-channel currents of the cone and the olfactory channel differ mainly in two features (see Table II): (i) the open time constant of the long opening mode is ~3 times larger in the olfactory channel than in the cone channel and (ii) the olfactory channel reveals short and long openings in the presence of cGMP and cAMP whereas the cone channel shows short and long openings in the presence of cGMP but only brief openings in the presence of cAMP. On a macroscopic scale, these differences in the single-channel current explain why the cone channel is only partially activated by cAMP whereas the olfactory channel reveals the same I_{max} with both cGMP and cAMP. The mutations introduced into the cone channel which give rise to Ch30 induce long openings also in the presence of cAMP, resulting in a substantial increase in the macroscopic current evoked by saturating concentrations of cAMP. Nevertheless, the duration of the long openings of Ch30 is still much shorter than those of the olfactory channel. Thus, the mutations present in Ch30 increase E_{cAMP} to a level which almost corresponds to that of E_{cGMP} in that channel but they do not transform the channel into an olfactory-like channel, which would have a much higher open probability for both cGMP and cAMP. Neither the ligand selectivity nor the voltage dependence of channel activation are significantly altered between Ch30 and CNG3. In addition, Ch30 and CNG3 contain the same CNBD, suggesting that the free energy change produced by cAMP binding may also be within the same range for both channel types. Thus, the mutations present in Ch30 may affect mainly the conformational step that couples the agonist binding with the channel opening. The observed increase in E_{cAMP} is explained by the fact that the energy barrier between the closed and open conformation is lowered in Ch30 with respect to that of CNG3. In summary, our data indicate that the three amino acids identified in the C-linker are major determinants of CNG channel gating.

Materials and methods

Molecular biology

For construction of chimeric CNG channels, the following plasmids were used: pCGK26/CMV containing the coding region of the bovine CNG3 α subunit, which was cloned originally from kidney (Biel *et al.*, 1994), and pCG357/CMV (Biel *et al.*, 1994) containing the coding region of the rabbit CNG2 subunit, which was cloned originally from rabbit aorta (former designation rACNG, Biel *et al.*, 1993). All chimeras were generated by standard PCR techniques and verified by sequencing. In Ch2, amino acids M1–M180 of CNG3 were replaced by M1–L133 of CNG2. In Ch3, amino acids S423–P706 of CNG3 were replaced by S376–P664. In Ch4, both M1–M180 and S423–P706 were replaced by the corresponding sequences of CNG2. In Ch8 and Ch9, amino acids S423–R536 and E537–P706 were replaced by the corresponding sequences of CNG2. The amino acids exchanged in CNG3 to generate

Ch12, 13, 20, 21, 24, 26, 28, 30 and 37 are indicated in Figure 3. The reverse chimera Ch25 was constructed by replacing amino acids V392–K489 of CNG2 by I439–R536 of CNG3. Additionally, the following mutations were made: Ch16, Q441H in CNG3; Ch17, H394Q in CNG2; Ch35, D481A, D494S in CNG3; Ch36, S428T in Ch30; Ch38, A520Q, K530R, R536K in Ch30. All constructs were transiently expressed in HEK293 cells as previously described (Biel *et al.*, 1994).

Electrophysiology

Macroscopic currents and single-channel currents were recorded from inside-out patches excised from human embryonic kidney (HEK) 293 cells by using a List EPC 7 amplifer and pCLAMP software (Axon Instruments). The patch pipettes with resistances of 2–3 MΩ (for single-channel recording 8–12 MΩ) were filled with Ringer solution containing 140 mM NaCl, 5.0 mM KCl, 10 mM HEPES, 1.0 mM EGTA, pH 7.4 adjusted with NaOH. A multi-barrelled perfusion pipette placed 200 µm away from the patch was used to switch the superfusion from Ringer solution to that containing agonists. If not stated otherwise, the membrane potential was held at 0 mV and stepped to ± 60 mV. Capacitive transients and leak currents were subtracted using currents recorded under the superfusion with Ringer solution without agonist. Data were digitized at 10 kHz, filtered at 2 kHz and analysed with AutesP (npi electronic GmbH). Dose–response curves for cGMP and cAMP alone were generated by measuring the current response at +60 mV and fitted with the Hill equation: $I/I_{max} = [C]^{\nu}/([C]^{\nu} + K_a^{\nu})$, where [C] is the cyclic nucleotide concentration, K_a is the activation constant and ν is the Hill coefficient. Dose–response curves of cGMP in the presence of cAMP were generated by measuring the current response at +60 mV and were fitted with a modified Dean equation (Dean, 1987): $E_{AB} = I_0((\alpha K_B[A] + \beta K_A[B])/(K_A[B] + K_B[A] + K_A K_B))$, where E_{AB} is the total effect of ligand A and B, I_0 is the normalized maximal current, K_A and K_B are the dissociation constants of ligand A and B, [A] and [B] are the concentration of ligand A and B and α and β are the efficacies of ligand A and B.

Single-channel data were analysed using a 50% amplitude criterion to detect opening and closing transitions. Open (τ_o) and closed (τ_c) time constants were calculated by fitting the dwell time histograms. Due to the experimental conditions, openings shorter than ~150 µs could not be resolved. Thus, the values of the measured time constants for brief openings and closings, τ_{01} and $\tau_{c1,}$ may be slightly larger than the real τ values.

All experiments were done at room temperature (20–22°C). All macroscopic currents represent mean values of the currents measured during the depolarizing step of 155 ms in order to minimize differences in currents because of an internal Na^+ depletion phenomenon that appeared particularly in patches with large currents (Zimmerman *et al.*, 1988). All values are given as mean ± SEM.

Acknowledgements

We thank P.Mayr, S.Stief, B.Lehnert and S.Ehrhard for excellent technical support. The research conducted in the author's laboratory was supported by grants from Fonds der Chemie and Deutsche Forschungsgemeinschaft.

References

Ahmad,I., Korbmacher,C., Segal,A.S., Cheung,P., Boulpaep,E.L. and Barnstable,C.J. (1992) Mouse cortical collecting duct cells show nonselective cation channel activity and express a gene related to the cGMP-gated rod photoreceptor channel. *Proc. Natl Acad. Sci. USA*, **89**, 10262–10266.

Altenhofen,W., Ludwig,J., Eismann,E., Kraus,W., Bönigk,W. and Kaupp,U.B. (1991) Control of ligand specificity in cyclic nucleotide-gated channels from rod photoreceptors and olfactory epithelium. *Proc. Natl Acad. Sci. USA*, **88**, 9868–9872.

Biel,M., Altenhofen,W., Hullin,R., Ludwig,J., Freichel,M., Flockerzi,V., Dascal,N., Kaupp,U.B. and Hofmann,F. (1993) Primary structure and functional expression of a cyclic nucleotide-gated channel from rabbit aorta. *FEBS Lett.*, **329**, 134–138.

Biel,M., Zong,X., Distler,M., Bosse,E., Klugbauer,N., Murakami,M., Flockerzi,V. and Hofmann,F. (1994) Another member of the cyclic nucleotide-gated channels family expressed in testis, kidney and heart. *Proc. Natl Acad. Sci. USA*, **91**, 3505–3509.

Biel,M., Zong,X. and Hofmann,F. (1995) Molecular diversity of cyclic nucleotide-gated cation channels. *Naunyn-Schmiedeberg's Arch. Pharmacol.*, **353**, 1–10.

Biel,M., Zong,X. and Hofmann,F. (1996) Cyclic nucleotide-gated cation channels. Molecular diversity, structure, and cellular functions. *Trends Cardiovasc. Med.*, **6**, 274–280.

Bönigk,W., Altenhofen,W., Müller,F., Dose,A., Illing,M., Molday,R.S. and Kaupp,U.B. (1993) Rod and cone photoreceptor cells express distinct genes for cGMP-gated channels. *Neuron*, **10**, 865–877.

Bönigk,W., Müller,F., Middendorff,R., Weyand,I. and Kaupp,U.B. (1996) Two alternatively spliced forms of the cGMP-gated channel α-subunit from cone photoreceptor are expressed in the chick pineal organ. *J. Neurosci.*, **16**, 7458–7468.

Bradley,J., Li,J., Davidson,N., Lester,H.A. and Zinn,K. (1994) Heteromeric olfactory cyclic nucleotide-gated channels: a new subunit that confers increased sensitivity to cAMP. *Proc. Natl Acad. Sci. USA*, **91**, 8890–8894.

Bradley,J., Zhang,Y., Bakin,R., Lester,H.A., Ronnett,G.V. and Zinn,K. (1997) Functional expression of the heteromeric 'olfactory' cyclic nucleotide-gated channel in the hippocampus: a potential effector of synaptic plasticity in brain neurons. *J. Neurosci.*, **17**, 1993–2005.

Broillet,M.C. and Firestein,S. (1996) Direct activation of the olfactory cyclic nucleotide-gated channel through modification of sulfhydryl groups by NO compounds. *Neuron*, **16**, 377–385.

Broillet,M.C. and Firestein,S. (1997) β subunits of the olfactory cyclic nucleotide-gated channel form a nitric oxide activated Ca^{2+} channel. *Neuron*, **18**, 951–958.

Chen,T.Y., Peng,Y.W., Dhallan,R.S., Ahamed,B., Reed,R.R. and Yau,K.W. (1993) A new subunit of the cyclic nucleotide-gated cation channel in retinal rods. *Nature*, **362**, 764–767.

Dean,P.M. (1987) The development of theories about drug–receptor interaction. In Dean,P.M. (ed.), *Molecular Foundations of Drug–Receptor Interaction.* Cambridge University Press, pp. 1–22.

Dhallan,R.S., Yau,K.W., Schrader,K.A. and Reed,R.R. (1990) Primary structure and functional expression of a cyclic nucleotide-activated channel from olfactory neurons. *Nature*, **347**, 184–187.

Distler,M., Biel,M., Flockerzi,V. and Hofmann,F. (1994) Expression of cyclic nucleotide-gated cation channels in non-sensory tissues and cells. *Neuropharmacology*, **33**, 1275–1282.

Dryer,S. and Henderson,D. (1991) A cyclic GMP-activated channel in dissociated cells of chick pineal gland. *Nature*, **353**, 756–758.

Fesenko,E.E., Kolesnikov,S.S. and Luyubarsky,A.L. (1985) Induction by cyclic GMP of cationic conductance in plasma membrane of retinal rod outer segments. *Nature*, **313**, 310–313.

Finn,J.T., Grunwald,M.E. and Yau,K.W. (1996) Cyclic nucleotide-gated ion channels: an extended family with diverse functions. *Annu. Rev. Physiol.*, **58**, 395–426.

Gordon,S.E. and Zagotta,W.N. (1995a) A histidine residue associated with the gate of the cyclic nucleotide-activated channels in rod photoreceptors. *Neuron*, **14**, 177–183.

Gordon,S.E. and Zagotta,W.N. (1995b) Localization of regions affecting an allosteric transition in cyclic nucleotide-activated channels. *Neuron*, **14**, 857–864.

Goulding,E.H., Ngai,J., Kramer,R.H., Colicos,S., Axel,R., Siegelbaum,S.A. and Chess,A. (1992) Molecular cloning and single-channel properties of the cyclic nucleotide-gated channel from catfish olfactory neurons. *Neuron*, **8**, 45–58.

Goulding,E.H., Tibbs,G.R. and Siegelbaum,S.A. (1994) Molecular mechanism of cyclic nucleotide-gated channel activation. *Nature*, **372**, 369–374.

Karlson,K.H., Ciampolillo-Bates,F., McCoy,D.E., Kizer,N.L. and Stanton,B.A. (1995) Cloning of a cGMP-gated cation channel from mouse kidney inner medullary collecting duct. *Biochim. Biophys. Acta*, **1236**, 197–200.

Kaupp,U.B. *et al.* (1989) Primary structure and functional expression from complementary DNA of the rod photoreceptor cyclic GMP-gated channel. *Nature*, **342**, 762–766.

Kingston,P.A., Zufall,F. and Barnstable,C.J. (1996) Rat hippocampal neurons express genes for both retinal and olfactory cyclic nucleotide-gated channels: novel targets for cAMP/cGMP function. *Proc. Natl Acad. Sci. USA*, **93**, 10440–10445.

Liman,E.R. and Buck,L.B. (1994) A second subunit of the olfactory cyclic nucleotide-gated channel confers high sensitivity to cAMP. *Neuron*, **13**, 611–621.

Liu,D.T., Tibbs,G.R. and Siegelbaum,S.A. (1996) Subunit stoichiometry of cyclic nucleotide-gated channels and effects of subunit order on channel function. *Neuron*, **16**, 983–990.

Nakamura,T. and Gold,G.H. (1987) A cyclic nucleotide-gated conductance in olfactory receptor cilia. *Nature*, **325**, 442–444.

Ruiz,M.L., London,B. and Nadal-Ginard,B. (1996) Cloning and characterization of an olfactory cyclic nucleotide-gated channel expressed in mouse heart. *J. Mol. Cardiol.*, **28**, 1453–1461.

Sautter,A., Biel,M. and Hofmann,F. (1997) Molecular cloning of cyclic nucleotide-gated cation channel subunits from pineal gland. *Mol. Brain Res.*, **47**, 171–175.

Shabb,J.B. and Corbin,J.D. (1992) Cyclic nucleotide-binding domains in proteins having diverse functions. *J. Biol. Chem.*, **267**, 5723–5726.

Tibbs,G.R., Goulding,E.H. and Siegelbaum,S.A. (1997) Allosteric activation and tuning of ligand efficacy in cyclic nucleotide-gated channels. *Nature*, **386**, 612–615.

Varnum,M.D. and Zagotta,W.N. (1996) Subunit interactions in the activation of cyclic nucleotide-gated ion channels. *Biophys. J.*, **70**, 2667–2679.

Varnum,M.D., Black,K.D. and Zagotta,W.N. (1995) Molecular mechanism for ligand discrimination of cyclic nucleotide-gated channels. *Neuron*, **15**, 619–625.

Weyand,I., Godde,M., Frings,S., Weiner,J., Müller,F., Altenhofen,W., Hatt,H. and Kaupp,U.B. (1994) Cloning and functional expression of a cyclic nucleotide-gated channel from mammalian sperm. *Nature*, **368**, 859–863.

Yau,K.W. and Nakatani,K. (1985) Light-suppressible, cyclic GMP-sensitive conductance in the plasma membrane of a truncated rod outer segment. *Nature*, **317**, 252–255.

Zagotta,W.N. and Siegelbaum,S.A. (1996) Structure and function of cyclic nucleotide-gated channels. *Annu. Rev. Neurosci.*, **19**, 235–263.

Zimmerman,A.L., Karpen,J.W. and Baylor,D.A. (1988) Hindered diffusion in excised membrane patches from retinal rod outer segments. *Biophys. J.*, **54**, 351–355.

Zufall,F., Firestein,S. and Shepherd.G.M. (1994) Cyclic nucleotide-gated ion channels and sensory transduction in olfactory receptor neurons. *Annu. Rev. Biophys. Biomol. Struct.*, **23**, 577–607.

Received September 12, 1997; revised October 28, 1997; accepted October 29, 1997